AD-A035 509 OHIO STATE UNIV COLUMBUS ELECTROSCIENCE LAB F/G 17/9
REDUCTION OF BACKSCATTERING BY IMPEDANCE LOADING.(U)
OCT 76 C W CHUANG F19628-72-C-0203
UNCLASSIFIED ESL-3424-6 RADC-TR-76-376 NL

1 OF 1
AD-A
035 509

END
DATE
FILMED
3-26-77
NTIS

U.S. DEPARTMENT OF COMMERCE
National Technical Information Service

AD-A035 509

REDUCTION OF BACKSCATTERING BY IMPEDANCE LOADING

Ohio State University
Columbus, Ohio

October 1976

ADA035509

RADC-TR-76-376
Interim Technical Report
October 1976

REDUCTION OF BACKSCATTERING BY IMPEDANCE LOADING

The Ohio State University

Approved for public release;
distribution unlimited

D D C
RECEIVED
FEB 11 1977
A

ROME AIR DEVELOPMENT CENTER
AIR FORCE SYSTEMS COMMAND
GRIFFISS AIR FORCE BASE, NEW YORK 13441

REPRODUCED BY
NATIONAL TECHNICAL
INFORMATION SERVICE
U. S. DEPARTMENT OF COMMERCE
SPRINGFIELD, VA. 22161

UNCLASSIFIED

SECURITY CLASSIFICATION OF THIS PAGE (When Data Entered)

REPORT DOCUMENTATION PAGE		READ INSTRUCTIONS BEFORE COMPLETING FORM
1. REPORT NUMBER RADC-TR-76-376	2. GOVT ACCESSION NO.	3. RECIPIENT'S CATALOG NUMBER
4. TITLE (and Subtitle) REDUCTION OF BACKSCATTERING BY IMPEDANCE LOADING		5. TYPE OF REPORT & PERIOD COVERED Interim Technical Report No.6
		6. PERFORMING ORG. REPORT NUMBER ESL 3424-6
7. AUTHOR(s) C. W. Chuang		8. CONTRACT OR GRANT NUMBER(s) F19628-72-C-0203
9. PERFORMING ORGANIZATION NAME AND ADDRESS The Ohio State University ElectroScience Laboratory, Department of Electrical Engineering Columbus, Ohio 43212		10. PROGRAM ELEMENT, PROJECT, TASK AREA & WORK UNIT NUMBERS 5635-02-04 61102F 681305
11. CONTROLLING OFFICE NAME AND ADDRESS Deputy for Electronic Technology (RADC/ETER) Hanscom AFB, MA 01731 Contract Monitor: Richard B. Mack, ETER		12. REPORT DATE October 1976
		13. NUMBER OF PAGES 40
14. MONITORING AGENCY NAME & ADDRESS(if different from Controlling Office)		15. SECURITY CLASS. (of this report) Unclassified
		15a. DECLASSIFICATION/DOWNGRADING SCHEDULE

16. DISTRIBUTION STATEMENT (of this Report)

Approved for public release; distribution unlimited.

17. DISTRIBUTION STATEMENT (of the abstract entered in Block 20, if different from Report)

18. SUPPLEMENTARY NOTES

19. KEY WORDS (Continue on reverse side if necessary and identify by block number)

nonspecular scattering
compensation theorem
impedance loading
cross section reduction

20. ABSTRACT (Continue on reverse side if necessary and identify by block number)

R uction of nonspecular backscatter from a thin square conducting plate with the leading edge parallel to the electric field by impedance loading is studied in this report. The plate is modeled with a wire-grid structure. With a thin-wire computer program for calculating the backscatter and a generalized compensation theorem, optimal lumped impedances can be chosen such that significant reductions of nonspecular backscatter can be achieved for plate sizes ranging from $L/\lambda=.1$ to $L/\lambda=1.4$.

DD FORM 1 JAN 73 1473 EDITION OF 1 NOV 65 IS OBSOLETE

UNCLASSIFIED

SECURITY CLASSIFICATION OF THIS PAGE (When Data Entered)

Professor D. L. Moffatt is the responsible investigator for this contract. Richard B. Mack (ETER), is the RADC Project Engineer.

This report has been reviewed by the RADC Information Office (OI) and is releasable to the National Technical Information Service (NTIS). At NTIS it will be releasable to the General public, including foreign nations.

This technical report has been reviewed and approved for publication.

APPROVED:

RICHARD B. MACK
Project Engineer

APPROVED: ALLAN C. SCHELL
Acting Chief
Electromagnetic Sciences Division

FOR THE COMMANDER:

Plans Office

CONTENTS

		Page
I.	TECHNICAL REPORTS ON CONTRACT F19628-72-C-0203	1
II.	PUBLICATIONS AND ORAL PRESENTATIONS ON CONTRACT F19628-72-C-0203	2
III.	INTRODUCTION	3
IV.	FORMULATION	3
V.	APPLICATIONS	12
VI.	CONCLUSION	35
REFERENCES		36

White Section
Buff Section
JUSTIFICATION
BY
DISTRIBUTION/AVAILABILITY CODES
Dist. AVAIL. and/or SPECIAL
A

I. TECHNICAL REPORTS ON CONTRACT F19628-72-C-0203

1. 3424-1: R. K. Mains and D. L. Moffatt, "Complex Natural Resonances of an Object in Detection and Discrimination," June 1974.

2. 3424-2: S. C. Lee, "Control of Electromagnetic Scattering by Antenna Impedance Loading," July 1974.

3. 3424-3: C. W. Chuang and D. L. Moffatt, "Complex Natural Resonances of Radar Targets via Prony's Method," April 1975.

4. 3424-4: Jon Anders Aas, "Control of Electromagnetic Scattering from Wing Profiles by Impedance Loading," July 1975.

5. 3424-5: D. L. Moffatt, R. C. Rudduck, C. W. Chuang, J. A. Aas, "Continuation of the Investigation of Multifrequency Radar Reflectivity and Radar Target Identification," July 1975.

6. 3424-6: C. W. Chuang, "Reduction of Backscattering by Impedance Loading," October 1976.

II. PUBLICATIONS AND ORAL PRESENTATIONS ON CONTRACT F19628-72-C-0203

1. D. L. Moffatt, J. H. Richmond and R. K. Mains, "Complex Natural Resonances of an Object in Detection and Discrimination," IEEE/G-AP Symposium and USNC/URSI Meeting, Boulder, Colorado, August 1973.

2. D. L. Moffatt and R. K. Mains, "Detection and Discrimination of Radar Targets," IEEE Transaction on Antennas and Propagation, Vol. AP-23, No. 3, May 1975, pp. 78-83.

3. C. W. Chuang and D. L. Moffatt, "Complex Natural Resonances of Radar Targets Via Prony's Method," 1975 International IEEE AP-s Symposium and USNC/URSI Meeting, June, 1975.

4. D. L. Moffatt and C. W. Chuang, "Discrimination of Radar Targets in the Presence of Noise," URSI, Boulder, Colorado, October 1975.

5. D. L. Moffatt, "Complex Natural Resonances of Radar Targets in Detection and Discrimination," RADC Conference on Use of SEM, invited speaker, October 1975.

6. D. L. Moffatt, "A New Approach to Space Object Identification," NORSIC 8, NORAD Space Craft Identification Conference, May 1976.

7. D. L. Moffatt and K. A. Shubert, "Natural Resonances Via Rational Approximants," Submitted to IEEE Transactions on Antennas and Propagation, June 1976.

8. D. L. Moffatt, "Complex Natural Resonances - State-of-the-Art and the Future," National Conference on Electromagnetic Scattering, June 1976.

9. C. W. Chuang and D. L. Moffatt, "Natural Resonances of Radar Targets Via Prony's Method and Target Discrimination," IEEE Transactions on Aerospace and Electronic Systems, AES-12, No. 5, September 1976.

10. D. L. Moffatt and C. W. Chuang, "Radar Target Identification," Short Course, 1976.

III. INTRODUCTION

Significant achievement on the reduction of nonspecular scattering over a large bandwidth has been reported in [1,2]. The reduction of nonspecular scattering was made possible by an impedance loading technique. A two-dimensional wing model was treated in both previous reports [1,2]. The reduction of nonspecular scattering from a thin square plate - a three-dimensional case was also treated in [1] but only for vertical polarization. The case of parallel polarization which was left unanswered in [1] and only briefly mentioned in [3] will be the task of the present report.

The mathematical complexity of the problem is solved numerically with the method of moments. The thin square plate is modeled with a wire-grid structure. The scattering is controlled by inserting variable lumped impedances. A general computer program for antenna and scattering problems involving thin wire structures developed by Richmond [4,5] is suitable for the present study. Though the calculation is in general complicated, the treatment of variable lumped impedances can be simplified with the compensation theorem. Formulations of the compensation theorem will be given in the next section. Section V is devoted to show that reduction of nonspecular scattering from a square plate for parallel polarization can be achieved by an impedance loading technique over a large bandwidth.

IV. FORMULATION

Calculations of the scattered fields from a conducting body loaded with variable lumped impedances can be simplified if the functional dependence of the scattered fields on the variable lumped impedances can be written explicitly in simple formulas. This can be done with the compensation theorem. In this section we shall expand the compensation theorem to include two variable lumped impedances.

From the theory of moment methods, the induced current on a scatterer modeled with a wire-grid structure can be expanded into several modes which satisfy the matrix equation

$$[Z_{mn}][I_n] = [V_m], \tag{1}$$

where Z is the square impedance matrix, I and V are column current and voltage matrices respectively. The exact expressions for Z_{mn} and V_m are well documented [4] and will not be presented here. If the scatterer is loaded with lumped impedances, the impedance matrix Z can be written as

$$Z_{mn} = \overline{Z}_{mn} + a_{mn} Z_{Lmn} \quad , \tag{2}$$

where $\overline{Z}$ is the impedance matrix without loading, Z_{Lmn} is the lumped load shared by current modes m and n, and the constant a_{mn} is defined by

$$a_{mn} = 1, \text{ if } I_m \text{ and } I_n \text{ are in the same direction,}$$
$$= -1, \text{ otherwise.}$$

To simplify the discussion, we shall consider only the case where no variable lumped impedances are shared by more than one current mode. In such a case, Equation (2) reduces to

$$Z_{mn} = \overline{Z}_{mn} + Z_m\delta_{mn}, \tag{3}$$

where δ_{mn} is a Kronecker delta and Z_m denotes a variable lumped impedance. In Equation (3) we have included those of fixed lumped impedances in $\overline{Z}$. Substituting Equation (3) into Equation (1),

$$[\overline{Z}_{mn}][I_n] = [V_m]-[Z_mI_m]. \tag{4}$$

Denoting the induced current modes on the scatterer when all the variable lumped impedances vanish as $\overline{I}_n$ and the difference between I_n and $\overline{I}_n$ as ΔI_n, then

$$[\overline{Z}_{mn}][\overline{I}_n] + [\overline{Z}_{mn}][\Delta I_n] = [V_m]-[Z_mI_m] \quad , \tag{5}$$

which can be split into two equations

$$[\overline{Z}_{mn}][\overline{I}_n] = [V_m], \tag{6}$$

$$[\overline{Z}_{mn}][\Delta I_n] = [-Z_mI_m]. \tag{7}$$

If both $\overline{I}$ and ΔI are known, the scattered fields can be calculated. The current $\overline{I}$ will radiate the scattered fields when all the variable lumped impedances on the scatterer vanish, while the current ΔI will radiate the excessive fields due to the effect of the variable lumped impedances. The latter is equivalent to the fields radiated when the scatterer is used as a transmitting antenna with an impressed voltage matrix $[-Z_mI_m]$ and with all the variable lumped impedances shorted. The total scattered electric field is

$$E = E^s + \sum_m \frac{-Z_mI_m}{Z_{am}} E_m^{\gamma}, \tag{8}$$

where E^s is the field radiated by $\bar{I}$ and the summation over m is due to ΔI. In Equation (8) Z_{am} is the antenna impedance and E_m^γ is the field radiated by the antenna when the driving terminals are at mode m having unit current through mode m. Both Z_{am} and E_m^γ are evaluated with all the variable lumped impedances shorted.

The antenna impedance Z_{am} can be found from Equation (6). Let $V_m = \delta_{m1}$, then

$$Z_{a1} = \frac{1}{I_1} = \frac{|\bar{Z}_{mn}|}{A_{11}} \quad , \tag{9}$$

where A_{11} is the cofactor of $\bar{Z}_{11}$ in the impedance matrix $[\bar{Z}_{mn}]$ and $|\bar{Z}_{mn}|$ is the determinant of $[\bar{Z}_{mn}]$. Similarly

$$Z_{am} = \frac{|\bar{Z}_{mn}|}{A_{mm}} \quad . \tag{10}$$

Next we shall express $[I_n]$ in terms of $[\bar{I}_n]$. To do this, we obtain from Equations (1) and (6)

$$[I_n] = [\bar{Z}_{mn} + Z_m\delta_{mn}]^{-1} \, [\bar{Z}_{mn}][\bar{I}_n]. \tag{11}$$

When Equation (11) is substituted into Equation (8), the functional dependence of the scattered field E on the variable lumped impedances is then explicitly given in Equation (8).

We shall examine Equation (8) in more detail for two simplest cases.

<u>A - Scatterer with one variable lumped impedance</u>:

From Equation (11),

$$[\bar{I}_n] = [\bar{Z}_{mn}]^{-1} \, [\bar{Z}_{mn} + Z_1\delta_{m1}\delta_{1n}][I_n]$$

$$= [I_n] + [\bar{Z}_{mn}]^{-1} \, [Z_1 I_1 \delta_{1n}],$$

and then

$$\bar{I}_1 = \left(1 + \frac{A_{11}Z_1}{|\bar{Z}_{mn}|}\right) I_1 = \left(1 + \frac{Z_1}{Z_{a1}}\right) I_1.$$

Therefore Equation (8) can be reduced to

$$E = E^S - \frac{Z_1}{Z_{a1}+Z_1} \bar{I}_1 E_1^Y \quad . \tag{12}$$

Let $E = E^X$ when $Z_1 = Z_1^X$. Then from Equation (12),

$$\bar{I}_1 E_1^Y = \frac{Z_{a1}+Z_1^X}{Z_1^X} (E^S - E^X). \tag{13}$$

Substituting Equation (13) into Equation (12), we have

$$E = \frac{Z_{a1}(Z_1^X - Z_1)E^S + Z_1(Z_{a1}+Z_1^X)E^X}{Z_1^X(Z_{a1}+Z_1)} \quad . \tag{14}$$

Because E and Z_{a1} are functions of Z_1, it is more appropriate to write Equation (14) as

$$E(Z_1) = \frac{Z_{a1}(o)(Z_1^X - Z_1)E(o) + Z_1[Z_{a1}(o)+Z_1^X]E(Z_1^X)}{Z_1^X[Z_{a1}(o)+Z_1]} \quad . \tag{15}$$

The argument of E and Z_{a1} refers to the value of Z_1. From Equation (15) it is seen that if E(o), $E(Z_1^X)$ and $Z_{a1}(o)$ are known, then the scattered field for different values of Z_1 can be calculated easily using Equation (15). If Z_1^X is set to be infinity, then Equation (15) can be simplified,

$$E(Z_1) = \frac{Z_{a1}(o)E(o) + Z_1 E(\infty)}{Z_{a1}(o)+Z_1} \quad . \tag{16}$$

<u>B - Scatterer with two variable lumped impedances</u>:

In this case we shall take a different approach. Instead of amplifying Equation (8), we start from Equation (15). Because there are two variable lumped impedances, both the scattered field E and the antenna impedance Z_a are functions of Z_1 and Z_2. From Equation (15)

$$E(Z_1,Z_2) = \frac{Z_{a1}(o,Z_2)(Z_1^X - Z_1)E(o,Z_2) + Z_1[Z_{a1}(o,Z_2)+Z_1^X]E(Z_1^X,Z_2)}{Z_1^X[Z_{a1}(o,Z_2)+Z_1]} \quad . \tag{17}$$

Similarly, we have

$$E(Z_1,Z_2) = \frac{Z_{a2}(Z_1,o)(Z_2^x-Z_2)E(Z_1,o)+Z_2[Z_{a2}(Z_1,o)+Z_2^x]E(Z_1,Z_2^x)}{Z_2^x[Z_{a2}(Z_1,o)+Z_2]} . \tag{18}$$

In Equations (17) and (18), the first argument of E and Z_a refers to the value of Z_1 and the second argument to that of Z_2.

In the following we shall write $E(o,Z_2)$, $E(Z_1^x,Z_2)$ and $Z_{a1}(o,Z_2)$ of Equation (17) as functions of Z_2 explicitly. This is easily done for $E(o,Z_2)$ and $E(Z_1^x,Z_2)$ by substituting $Z_1=0$ and $Z_1=Z_1^x$ into Equation (18), respectively,

$$E(o,Z_2) = \frac{Z_{a2}(o,o)(Z_2^x-Z_2)E(o,o)+Z_2[Z_{a2}(o,o)+Z_2^x]E(o,Z_2^x)}{Z_2^x[Z_{a2}(o,o)+Z_2]} , \tag{19}$$

$$E(Z_1^x,Z_2) = \frac{Z_{a2}(Z_1^x,o)(Z_2^x-Z_2)E(Z_1^x,o)+Z_2[Z_{a2}(Z_1^x,o)+Z_2^x]E(Z_1^x,Z_2^x)}{Z_2^x[Z_{a2}(Z_1^x,o)+Z_2]} . \tag{20}$$

For $Z_{a1}(o,Z_2)$, we proceed as follows: The antenna is viewed as a two-port network as shown in Figure 1. Referring to Figure 1, we can write down the following equations immediately,

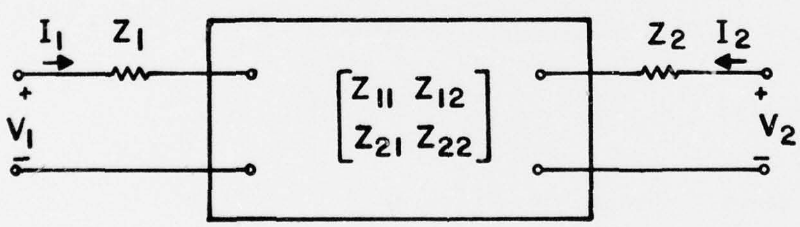

Figure 1. Antenna with lumped impedances viewed as a two-port network.

$$V_1 = I_1(Z_{11}+Z_1) + I_2Z_{12}, \tag{21}$$

$$V_2 = I_1Z_{21} + I_2(Z_{22}+Z_2), \tag{22}$$

$$Z_{a1}(o,Z_2^x) = \left.\frac{V_1}{I_1}\right|_{\substack{V_2=0\\ Z_1=0\\ Z_2=Z_2^x}} = Z_{11} - \frac{Z_{12}Z_{21}}{Z_{22}+Z_2^x} , \tag{23}$$

$$Z_{a1}(o,o) = \left.\frac{V_1}{I_1}\right|_{\substack{V_2=0\\ Z_1=0\\ Z_2=0}} = Z_{11} - \frac{Z_{12}Z_{21}}{Z_{22}} , \tag{24}$$

$$Z_{a2}(Z_1^x,o) = \left.\frac{V_2}{I_2}\right|_{\substack{V_1=0\\ Z_1=Z_1^x\\ Z_2=0}} = Z_{22} - \frac{Z_{12}Z_{21}}{Z_{11}+Z_1^x} , \tag{25}$$

$$Z_{a2}(o,o) = \left.\frac{V_2}{I_2}\right|_{\substack{V_1=0\\ Z_1=0\\ Z_2=0}} = Z_{22} - \frac{Z_{12}Z_{21}}{Z_{11}} . \tag{26}$$

From Equations (23) through (26) we can solve Z_{11}, Z_{12}, Z_{21} and Z_{22} in terms of $Z_{a1}(o,Z_2^x)$, $Z_{a1}(o,o)$, $Z_{a2}(Z_1^x,o)$ and $Z_{a2}(o,o)$. Rewriting Equations (23) through (26),

$$Z_{11}Z_{22} - Z_{12}Z_{21} + Z_{11}Z_2^x = (Z_{22}+Z_2^x)\ Z_{a1}(o,Z_2^x), \tag{27}$$

$$Z_{11}Z_{22} - Z_{12}Z_{21} = Z_{22}Z_{a1}(o,o), \tag{28}$$

$$Z_{11}Z_{22} - Z_{12}Z_{21} + Z_{22}Z_1^x = (Z_{11}+Z_1^x)\ Z_{a2}(Z_1^x,o), \tag{29}$$

$$Z_{11}Z_{22} - Z_{12}Z_{21} = Z_{11}Z_{a2}(o,o). \tag{30}$$

From Equations (28) and (29), we obtain

$$Z_{22}Z_{a1}(o,o) + Z_{22}Z_1^x = (Z_{11}+Z_1^x)\ Z_{a2}(Z_1^x,o),$$

or

$$Z_{11} = \frac{Z_{22}[Z_{a1}(o,o)+Z_1^x]}{Z_{a2}(Z_1^x,o)} - Z_1^x \quad . \tag{31}$$

Substituting Equations (28) and (31) into Equation (27),

$$Z_{22}Z_{a1}(o,o) + \left\{ \frac{Z_{22}[Z_{a1}(o,o)+Z_1^x]}{Z_{a2}(Z_1^x,o)} - Z_1^x \right\} Z_2^x = (Z_{22}+Z_2^x)Z_{a1}(o,Z_2^x).$$

From this equation we solve for Z_{22},

$$Z_{22} = \frac{Z_2^x Z_{a2}(Z_1^x,o)[Z_{a1}(o,Z_2^x)+Z_1^x]}{Z_2^x[Z_{a1}(o,o)+Z_1^x]+Z_{a2}(Z_1^x,o)[Z_{a1}(o,o)-Z_{a1}(o,Z_2^x)]} \quad . \tag{32}$$

Rewriting Equation (28) in the following form,

$$Z_{12}Z_{21} = Z_{11}Z_{22} - Z_{22}Z_{a1}(o,o). \tag{33}$$

Therefore Equations (31) through (33) can be used to solve for Z_{22}, Z_{11}, and $Z_{12}Z_{21}$ in terms of $Z_{a1}(o,o)$, $Z_{a1}(o,Z_2^x)$ and $Z_{a2}(Z_1^x,o)$. When this is done, then from Equation (23) we arrive at

$$Z_{a1}(o,Z_2) = Z_{11} - \frac{Z_{12}Z_{21}}{Z_{22}+Z_2} \quad , \tag{34}$$

which expresses the antenna impedance $Z_{a1}(o,Z_2)$ in terms of the network parameters and the variable lumped impedance Z_2. A simple formula relating the antenna impedances $Z_{a1}(o,o)$ and $Z_{a2}(o,o)$ can be derived from Equations (28) and (30).

$$Z_{a2}(o,o) = \frac{Z_{22}}{Z_{11}} Z_{a1}(o,o). \tag{35}$$

This completes the derivation of the formulas. To recount the formulas, we have

$$E(Z_1,Z_2) = \frac{Z_{a1}(o,Z_2)(Z_1^x-Z_1)E(o,Z_2)+Z_1[Z_{a1}(o,Z_2)+Z_1^x]E(Z_1^x,Z_2)}{Z_1^x[Z_{a1}(o,Z_2)+Z_1]}, \tag{17}$$

$$E(o,Z_2) = \frac{Z_{a2}(o,o)(Z_2^x-Z_2)E(o,o)+Z_2[Z_{a2}(o,o)+Z_2^x]E(o,Z_2^x)}{Z_2^x[Z_{a2}(o,o)+Z_2]}, \tag{19}$$

$$E(Z_1^x,Z_2) = \frac{Z_{a2}(Z_1^x,o)(Z_2^x-Z_2)E(Z_1^x,o)+Z_2[Z_{a2}(Z_1^x,o)+Z_2^x]E(Z_1^x,Z_2^x)}{Z_2^x[Z_{a2}(Z_1^x,o)+Z_2]}, \tag{20}$$

$$Z_{a1}(o,Z_2) = Z_{11} - \frac{Z_{12}Z_{21}}{Z_{22}+Z_2}, \tag{34}$$

$$Z_{12}Z_{21} \doteq Z_{22}[Z_{11} - Z_{a1}(o,o)], \tag{33}$$

$$Z_{a2}(o,o) = \frac{Z_{22}}{Z_{11}} Z_{a1}(o,o), \tag{35}$$

$$Z_{11} = \frac{Z_{22}[Z_{a1}(o,o) + Z_1^x]}{Z_{a2}(Z_1^x,o)} - Z_1^x, \tag{31}$$

$$Z_{22} = \frac{Z_2^x Z_{a2}(Z_1^x,o)[Z_{a1}(o,Z_2^x) + Z_1^x]}{Z_2^x[Z_{a1}(o,o) + Z_1^x] + Z_{a2}(Z_1^x,o)[Z_{a1}(o,o) - Z_{a1}(o,Z_2^x)]}. \tag{32}$$

From these equations, i.e., Equations (17), (19), (20), (34), (33), (35), (31) and (32), it is seen that if the values of $Z_{a1}(o,o)$, $Z_{a1}(o,Z_2^x)$, $Z_{a2}(Z_1^x,o)$, $E(o,o)$, $E(o,Z_2^x)$, $E(Z_1^x,o)$ and $E(Z_1^x,Z_2^x)$ are known, then the scattered field $E(Z_1,Z_2)$ for arbitrary values of Z_1 and Z_2 can be easily calculated through these equations. This method is especially efficient if the scattered fields for many different values of Z_1 and Z_2 are to be calculated.

From the above formulas, simpler but not necessarily more efficient formulas can be derived by setting $Z_1^x = Z_2^x = \infty$,

$$Z_{22} = Z_{a2}(\infty,o), \tag{36}$$

$$Z_{11} = Z_{a1}(o,\infty), \tag{37}$$

$$Z_{a2}(o,o) = \frac{Z_{a2}(\infty,o)}{Z_{a1}(o,\infty)} Z_{a1}(o,o), \tag{38}$$

$$Z_{12}Z_{21} = Z_{a2}(\infty,o)[Z_{a1}(o,\infty) - Z_{a1}(o,o)], \tag{39}$$

$$Z_{a1}(o,Z_2) = \frac{Z_{a1}(o,\infty)[Z_{a2}(o,o)+Z_2]}{Z_{a2}(\infty,o)+Z_2}, \tag{40}$$

$$E(\infty,Z_2) = \frac{Z_{a2}(\infty,o)E(\infty,o)+Z_2E(\infty,\infty)}{Z_{a2}(\infty,o)+Z_2}, \tag{41}$$

$$E(o,Z_2) = \frac{Z_{a2}(o,o)E(o,o)+Z_2E(o,\infty)}{Z_{a2}(o,o)+Z_2}, \tag{42}$$

$$E(Z_1,Z_2) = \frac{Z_{a1}(o,Z_2)E(o,Z_2)+Z_1E(\infty,Z_2)}{Z_{a1}(o,Z_2)+Z_1}. \tag{43}$$

Applications of the formulas derived here will be given in the next section.

V. APPLICATIONS

As shown in Figure 2, a thin square conducting plate slotted on

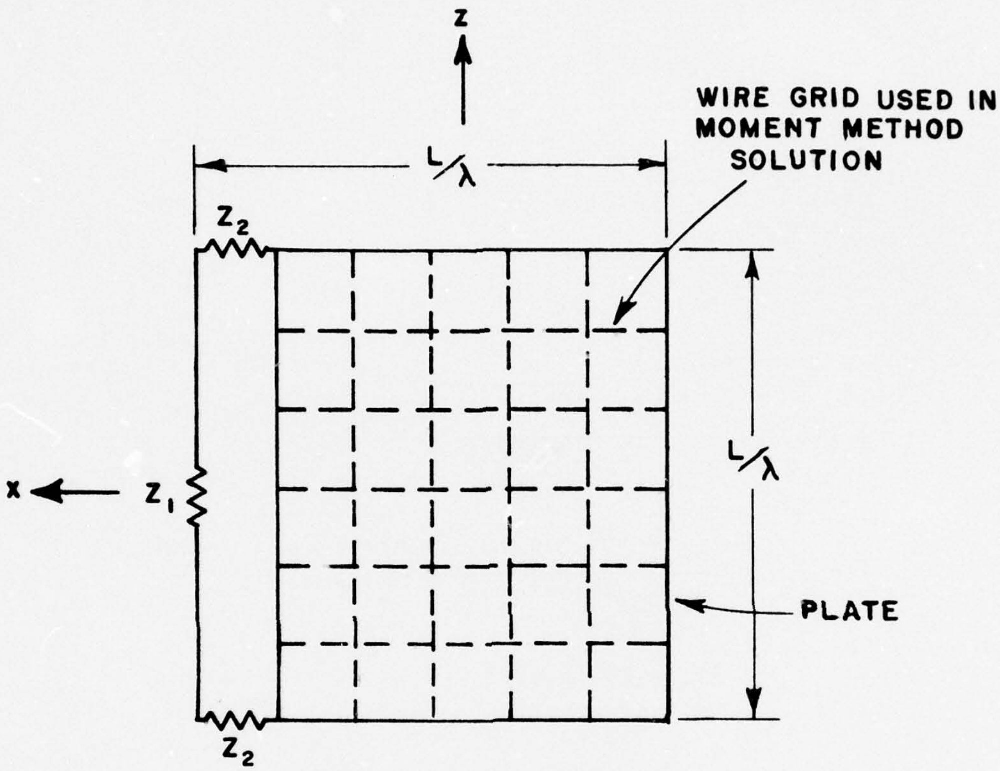

Figure 2. Wire grid model of folded dipole geometry.

one side is modeled with a wire-grid structure. Lumped impedances of values Z_1 and Z_2 are inserted on the slotted side. The purpose here is to optimize the impedances Z_1 and Z_2 such that significant reduction of the backscatter from the slotted plate can be achieved at near grazing incidence with electric field polarized parallel to the slot. Although there are three lumped impedances (Z_1, Z_2, Z_2), the formulas for the case of two lumped impedances derived in the previous section can still be used if the symmetry property of the structure is employed.

From folded dipole theory*, Z_2 is chosen to be pure reactive. However, Z_1 can have resistance. We first calculate the antenna

*The author is indebted to Professor L. Peters, Jr. for many discussions of the folded dipole theory.

impedances $Z_{a1}(o,o)$, $Z_{a1}(o,Z_2^x)$, $Z_{a2}(Z_1^x,o)$ and the backscattered fields $E(o,o)$, $E(o,Z_2^x)$, $E(Z_1^x,o)$, $E(Z_1^x,Z_2^x)$ using a computer program developed by Richmond [5]*. Then varying the values of Z_1 and Z_2 and calculating the backscattered field $E(Z_1,Z_2)$ using the formulas derived in the previous section, we obtain a figure of merit as the sum of the echo areas at $\phi=0°,10°,20°,30°,40°$. The computer is programmed to select the load impedances yielding the smallest figures of merit. The optimal values of Z_1 and Z_2 are then determined. The results are shown in Figures 3 through 16. Both echo areas for unslotted plates and slotted plates with optimal Z_1 and Z_2 are presented. From these figures it is seen that the reduction of backscatter at near grazing incidence can be achieved for plate sizes ranging from $L/\lambda=.1$ to $L/\lambda=1.4$. The size of $L/\lambda=1.4$ is not a restriction on the target size but merely one introduced by the core of the computer being used to make these computations. The optimal impedances Z_1 and Z_2 for minimizing the backscatter at near grazing incidence are summarized in Figures 17 and 18. The problem of how to implement the impedances is not dealt with at this time. However it is observed that Z_2 is the impedance required to reflect an open circuit across the antenna for the asymmetrical current mode at the position of the input terminals of the folded dipole. This could be realized at a single frequency by placing a short circuit (shorted diode) across the antenna at the proper place. The impedance Z_1 would appear to be physically realizable over most of the frequency band. Thus, the echo reduction suggested can be achieved using an adaptive system where the frequency of the incoming radar is sensed and the appropriate diode would be activated.

With optimal impedance loading which reduces the backscatter at grazing incidence we expect that the induced current will redistribute itself on the plate. As shown in Figures 19 and 20, the current on an unslotted square plate of size $L/\lambda=.2$ induced by a plane wave of parallel polarization at grazing incidence is compared to that induced on a plate of the same size with optimal impedance loading. The change of the induced current at the leading edge (slotted edge) is large. The total current in the z-direction is reduced when the plate is loaded with optimal impedances.

Impedance loading may find applications in the study of target discrimination. In one technique of target discrimination the natural resonances of a target are important parameters [6,7]. Therefore, it is interesting to ask if impedance loading of a target will alter the natural resonances of the target drastically. For the square plate studied in this section the dominant natural resonances can be obtained

---

*The author is indebted to Professor J. H. Richmond for the use of his computer program.

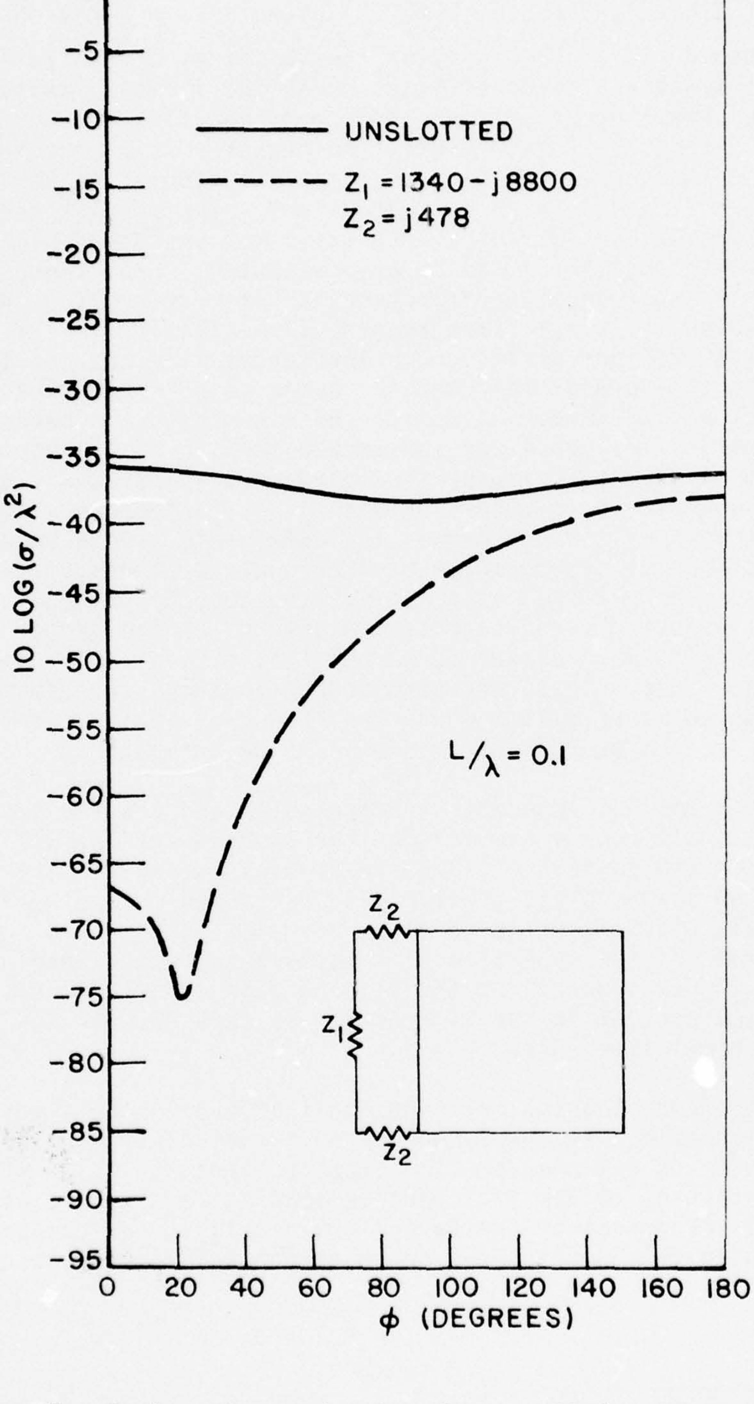

Figure 3. Backscatter reduction for parallel polarization.

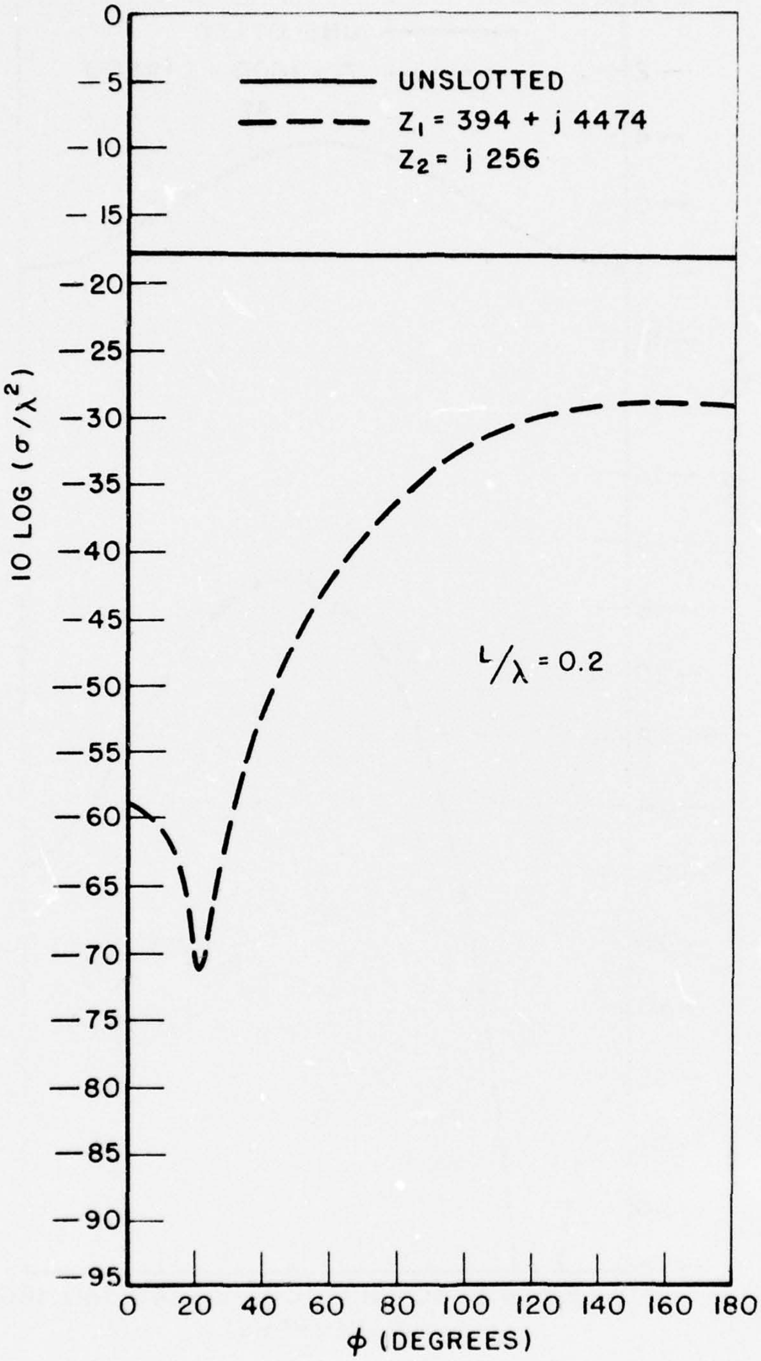

Figure 4. Backscatter reduction for parallel polarization.

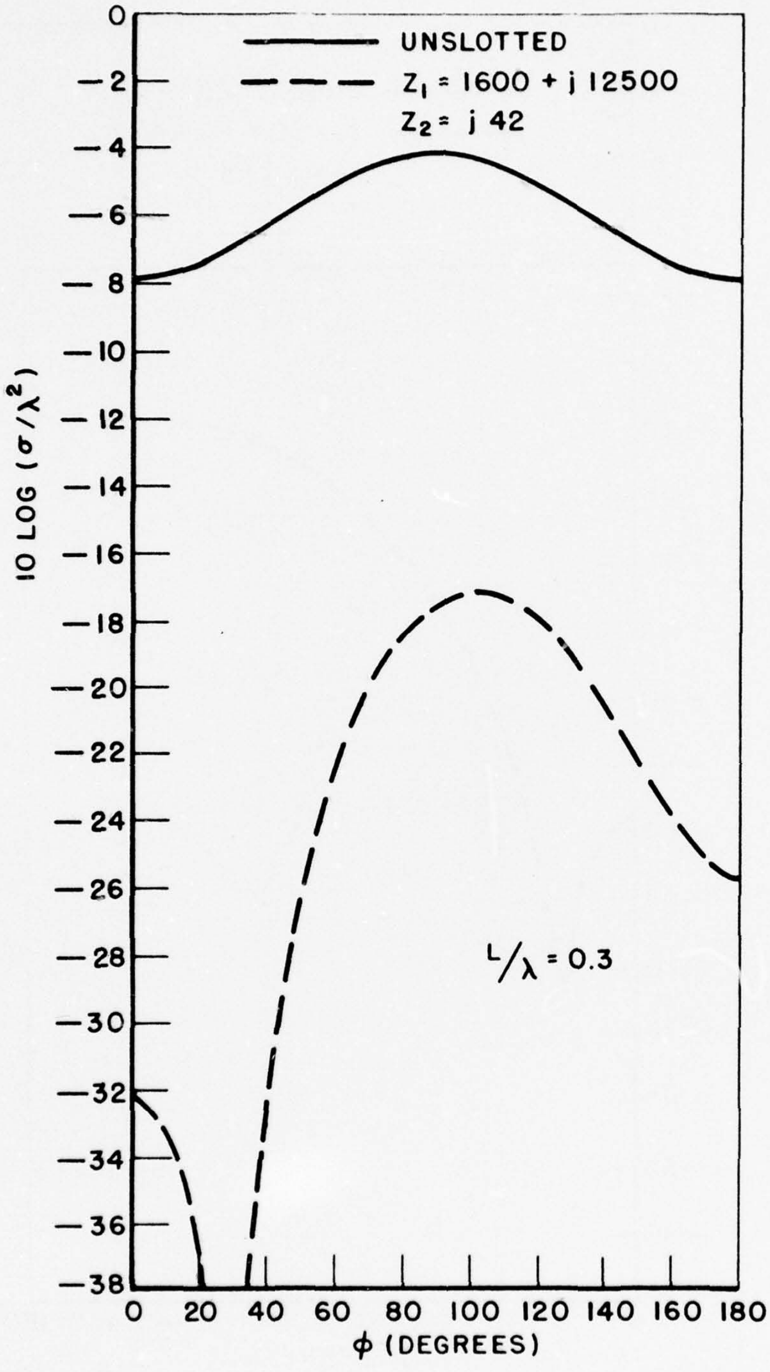

Figure 5. Backscatter reduction for parallel polarization.

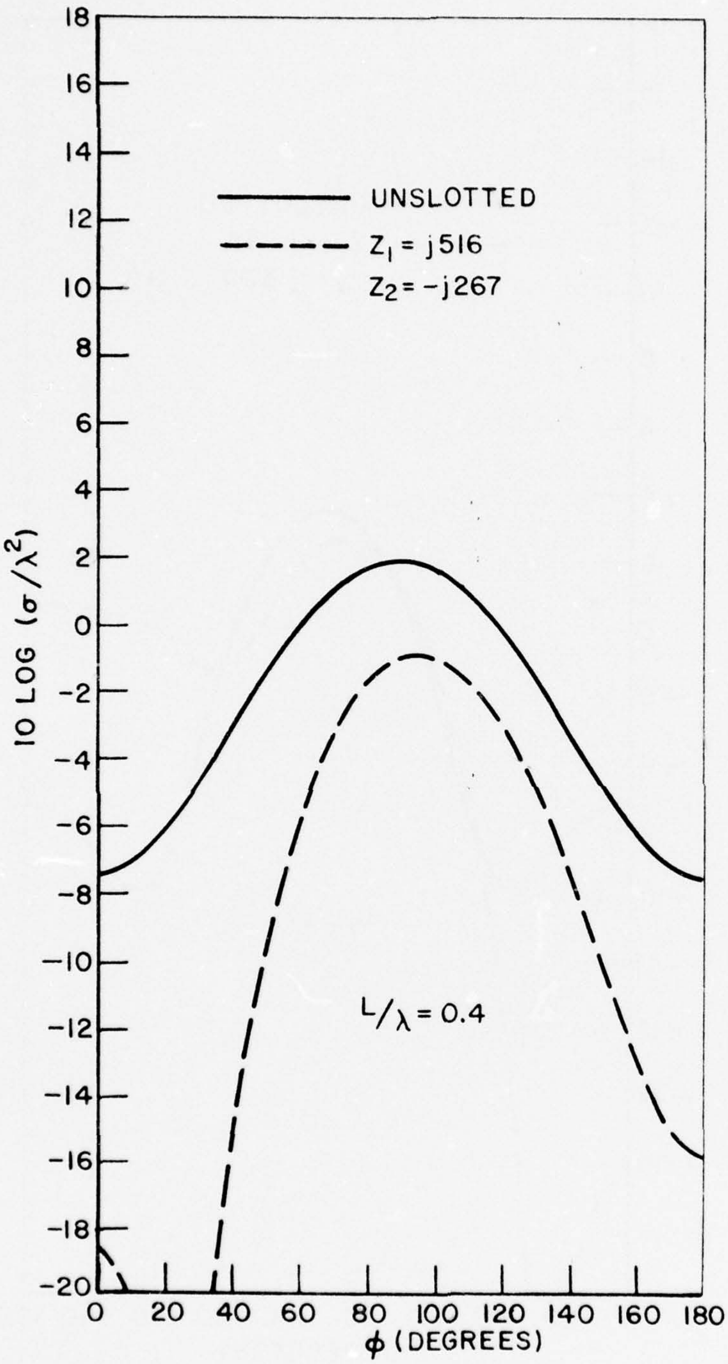

Figure 6. Backscatter reduction for parallel polarization.

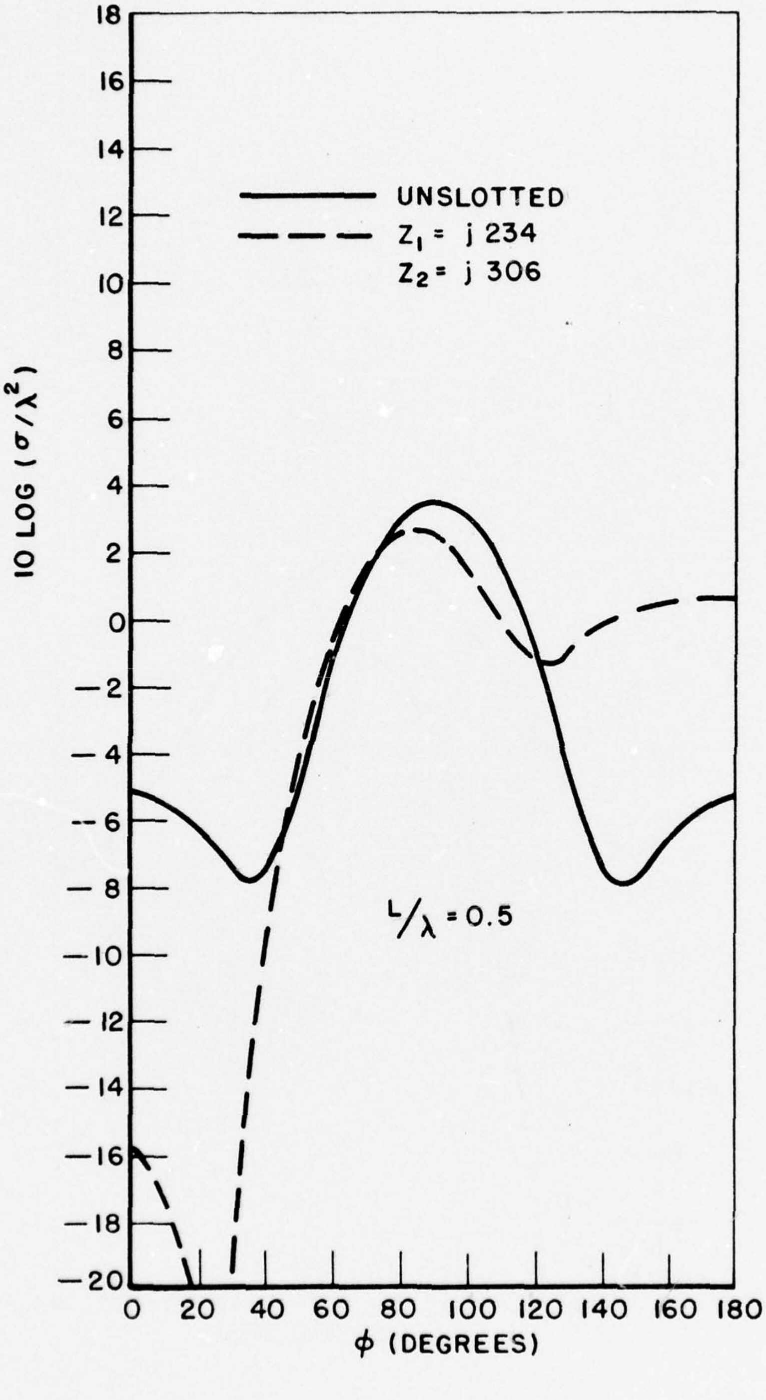

Figure 7. Backscatter reduction for parallel polarization.

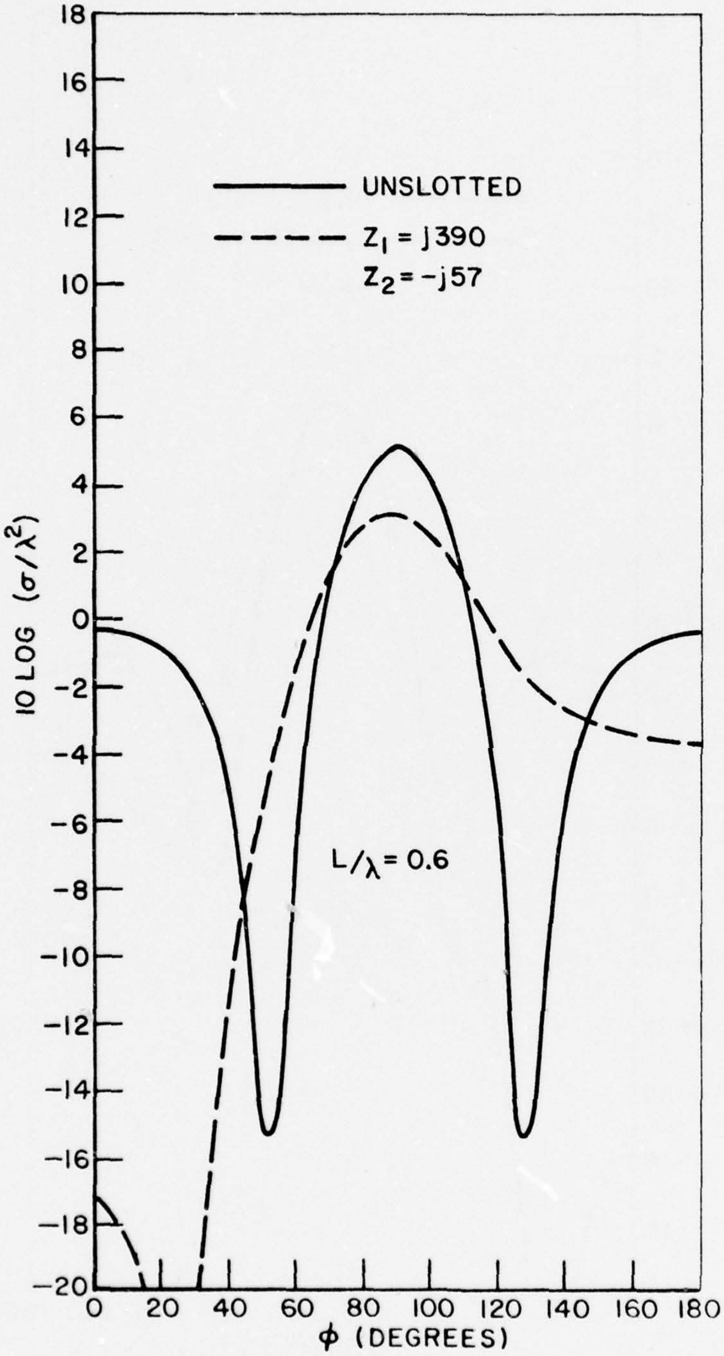

Figure 8. Backscatter reduction for parallel polarization.

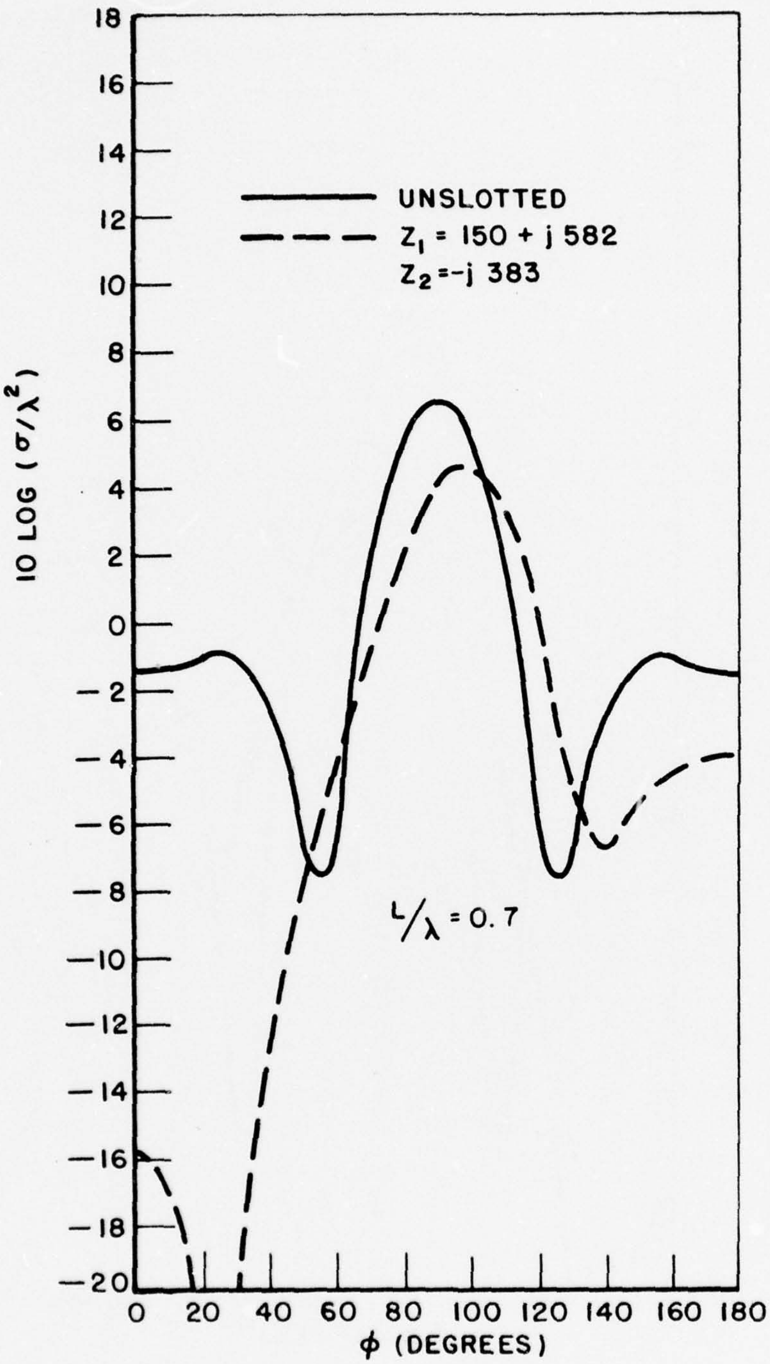

Figure 9. Backscatter reduction for parallel polarization.

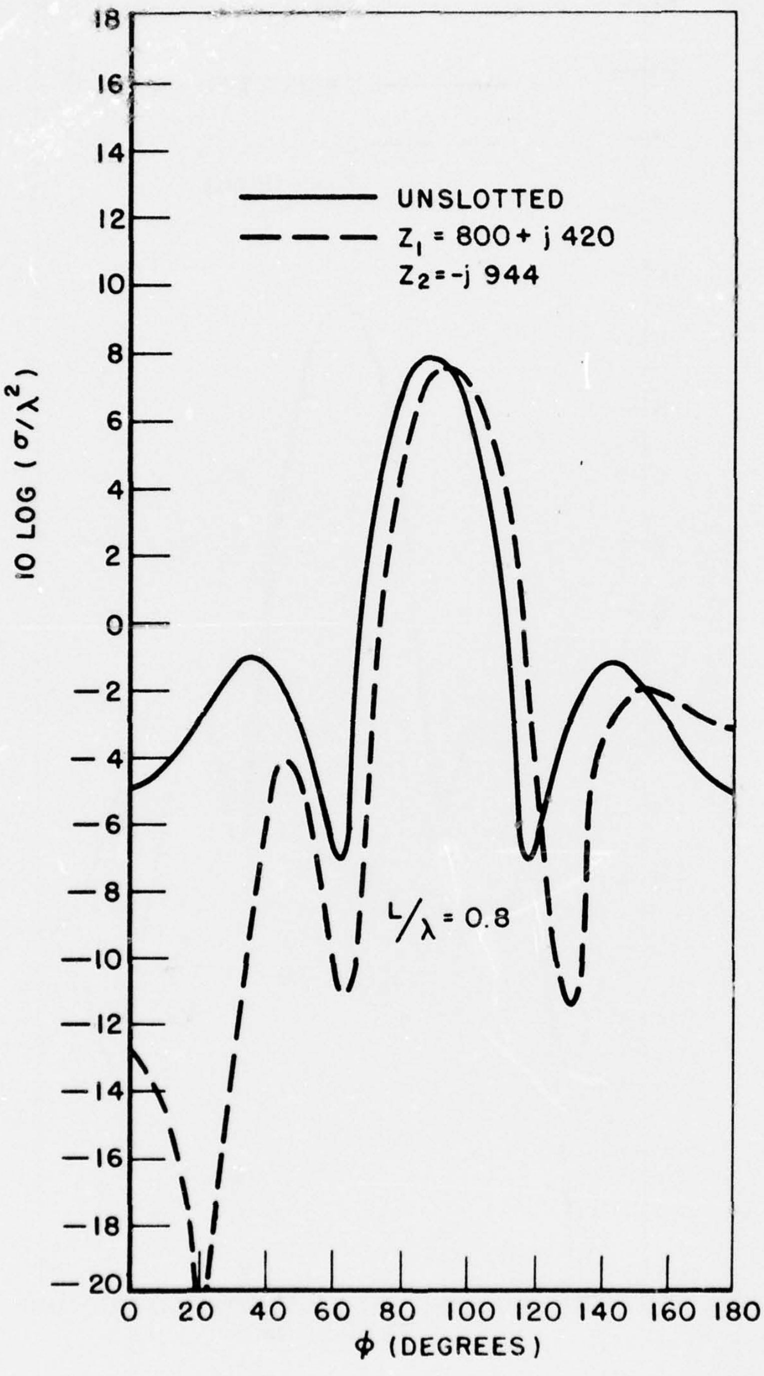

Figure 10. Backscatter reduction for parallel polarization.

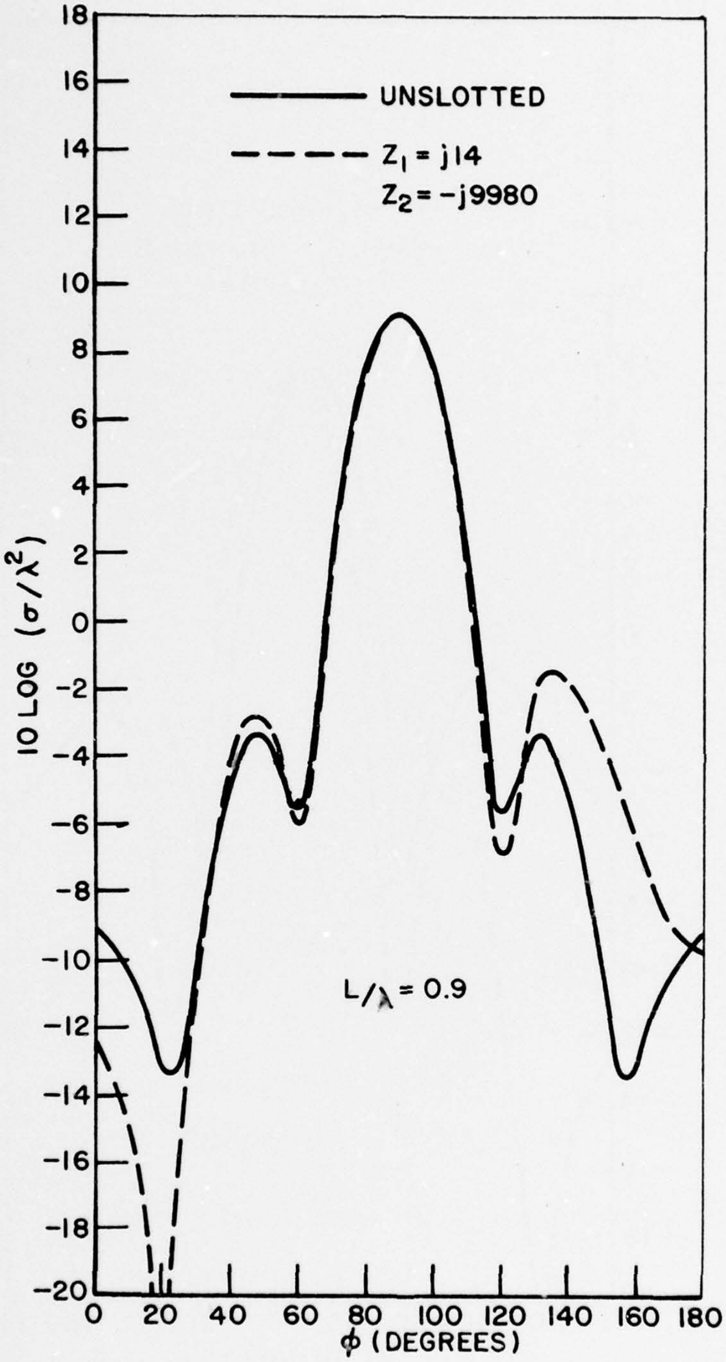

Figure 11. Backscatter reduction for parallel polarization.

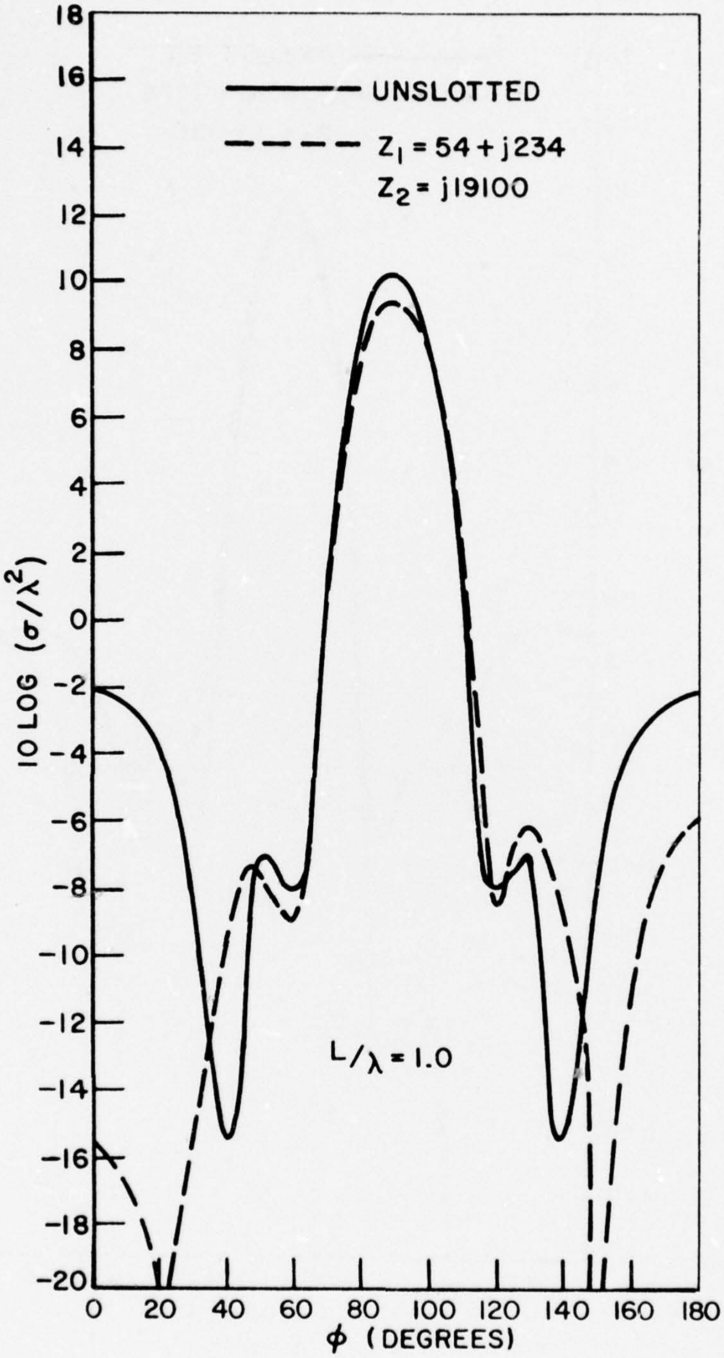

Figure 12. Backscatter reduction for parallel polarization.

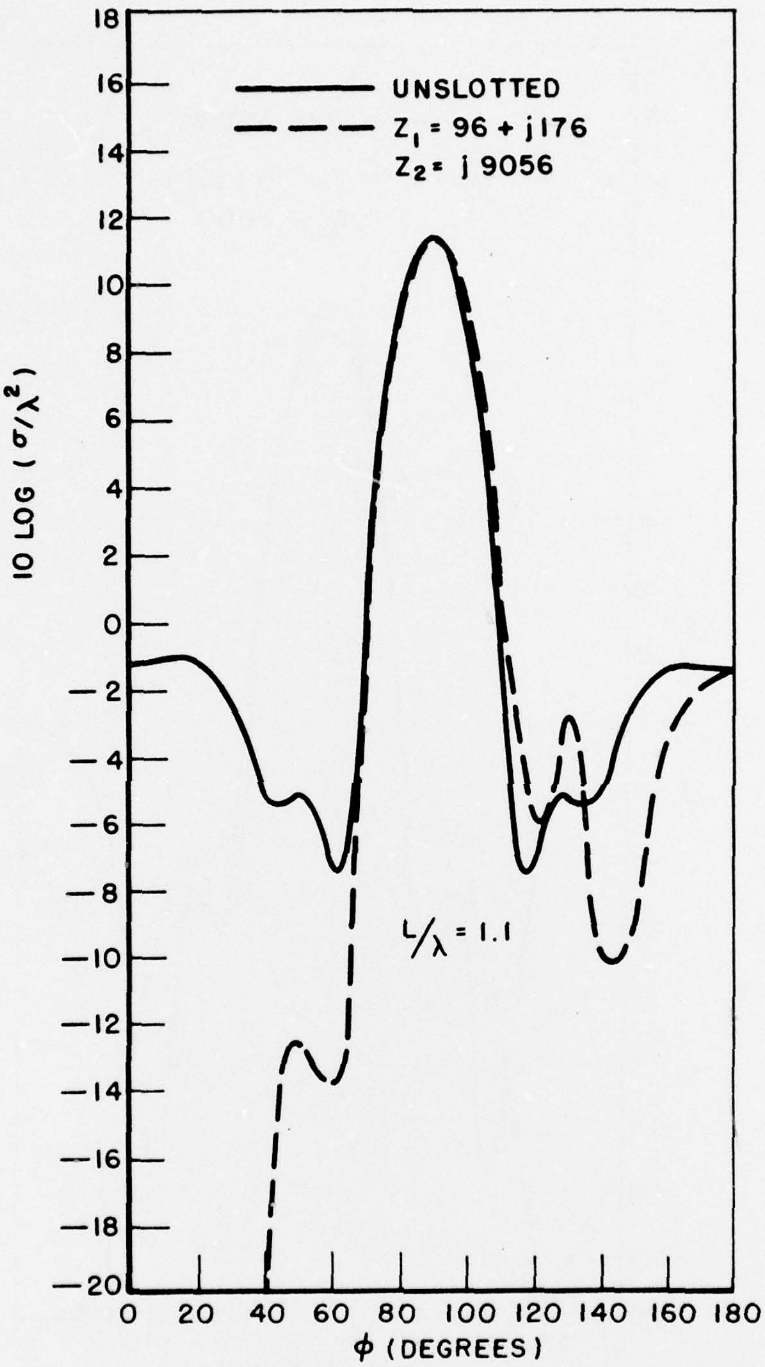

Figure 13. Backscatter reduction for parallel polarization.

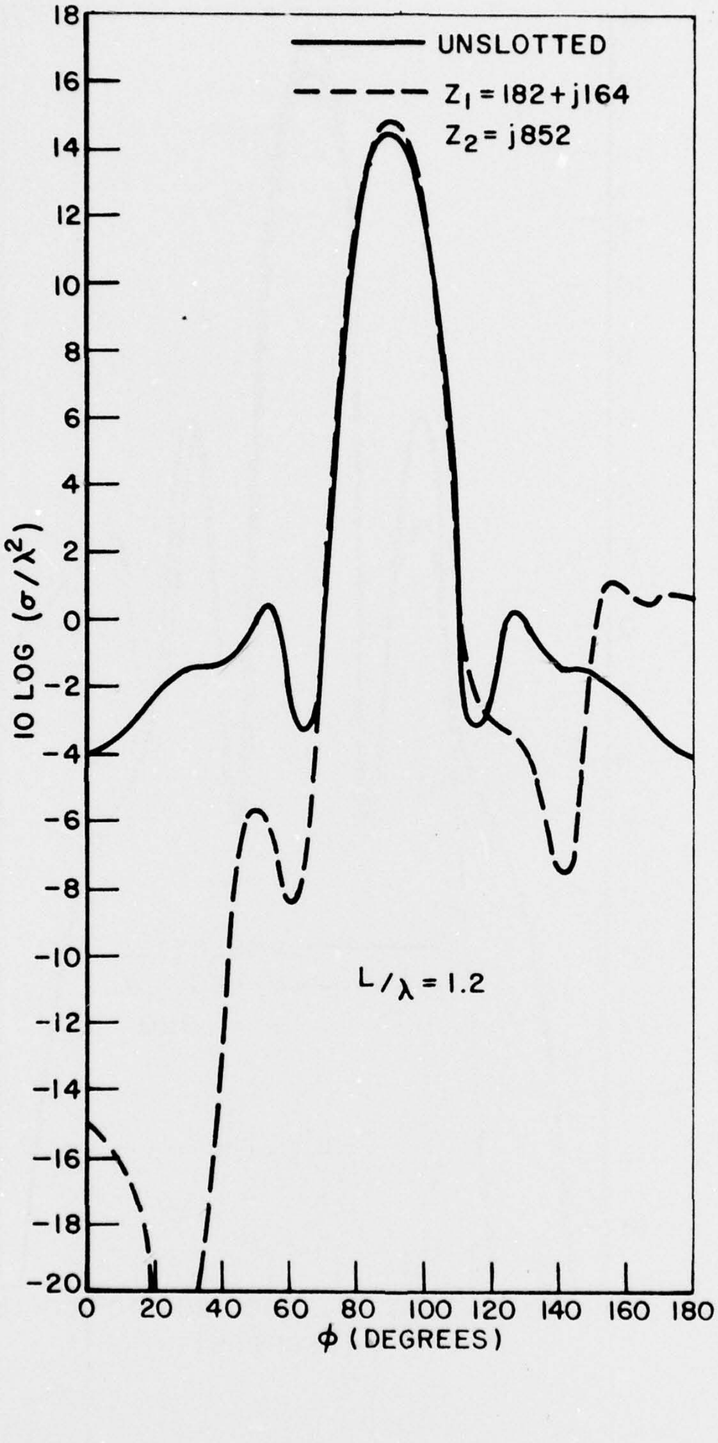

Figure 14. Backscatter reduction for parallel polarization.

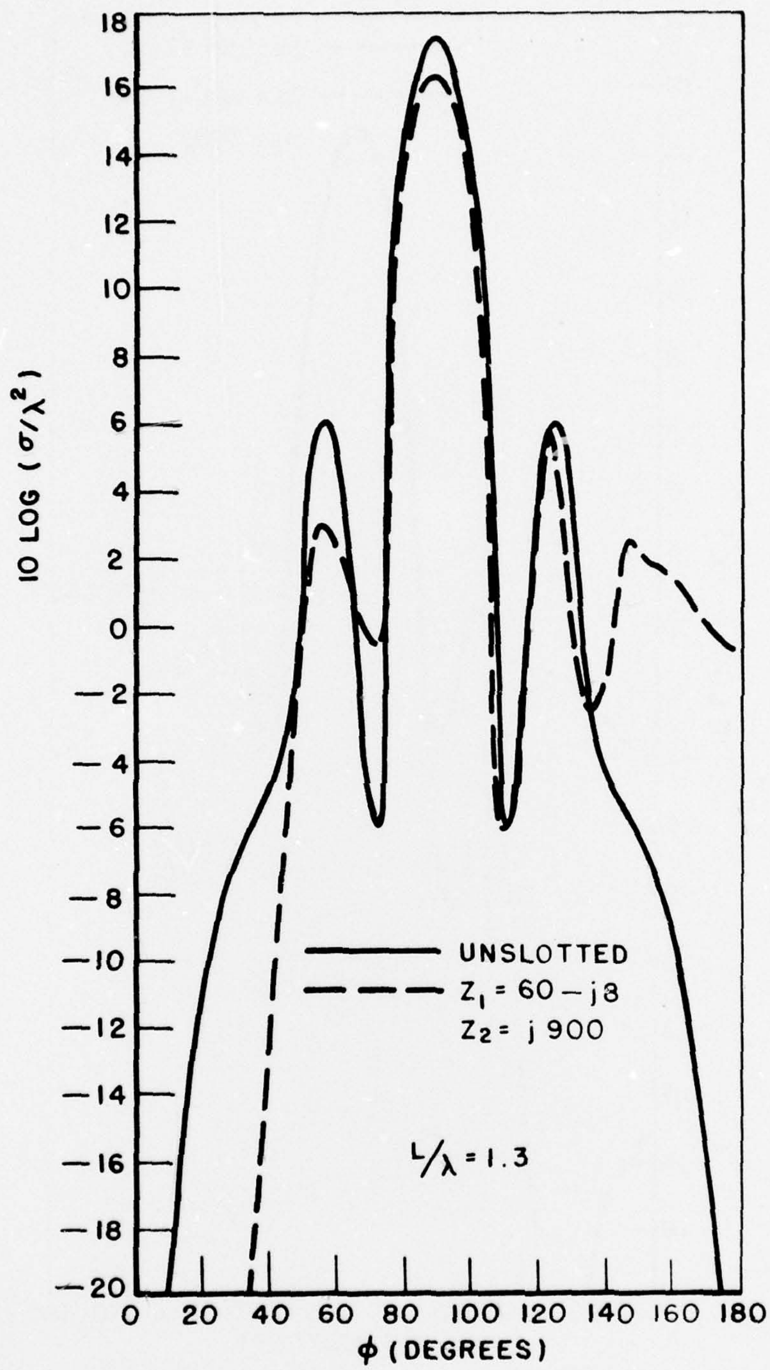

Figure 15. Backscatter reduction for parallel polarization.

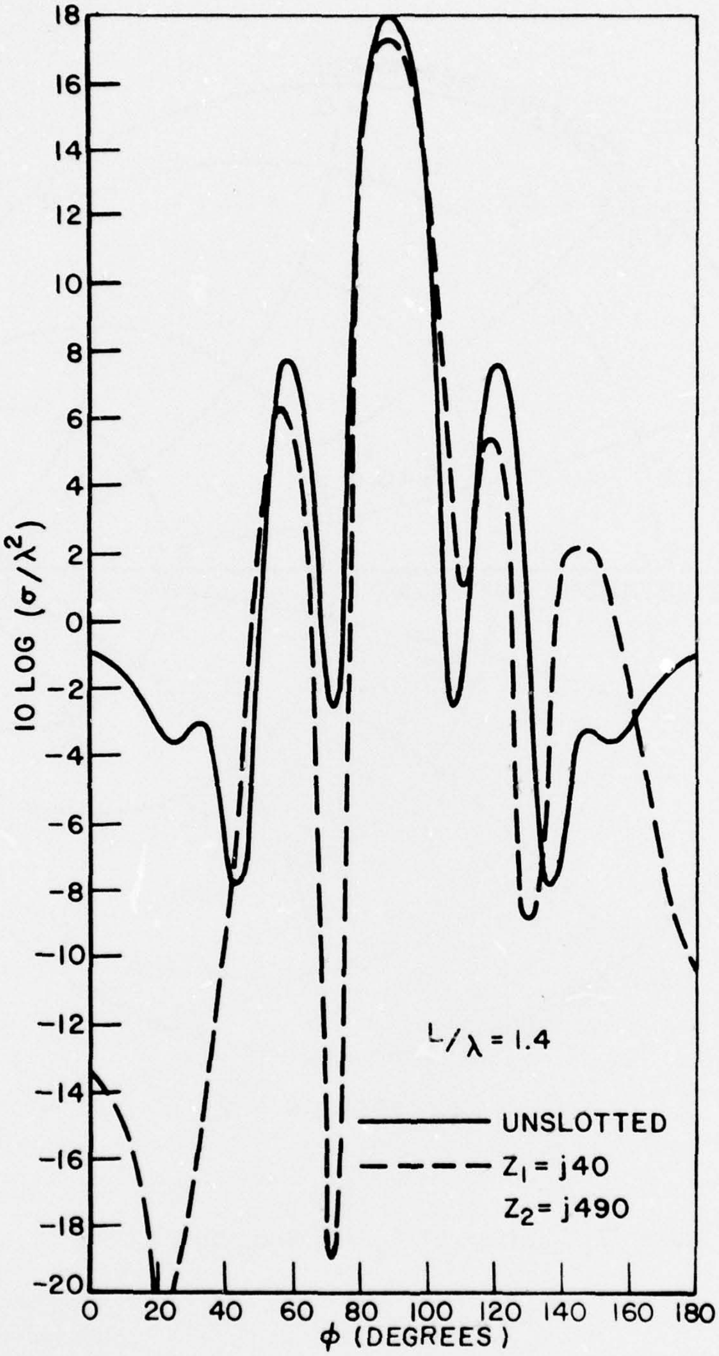

Figure 16. Backscatter reduction for parallel polarization.

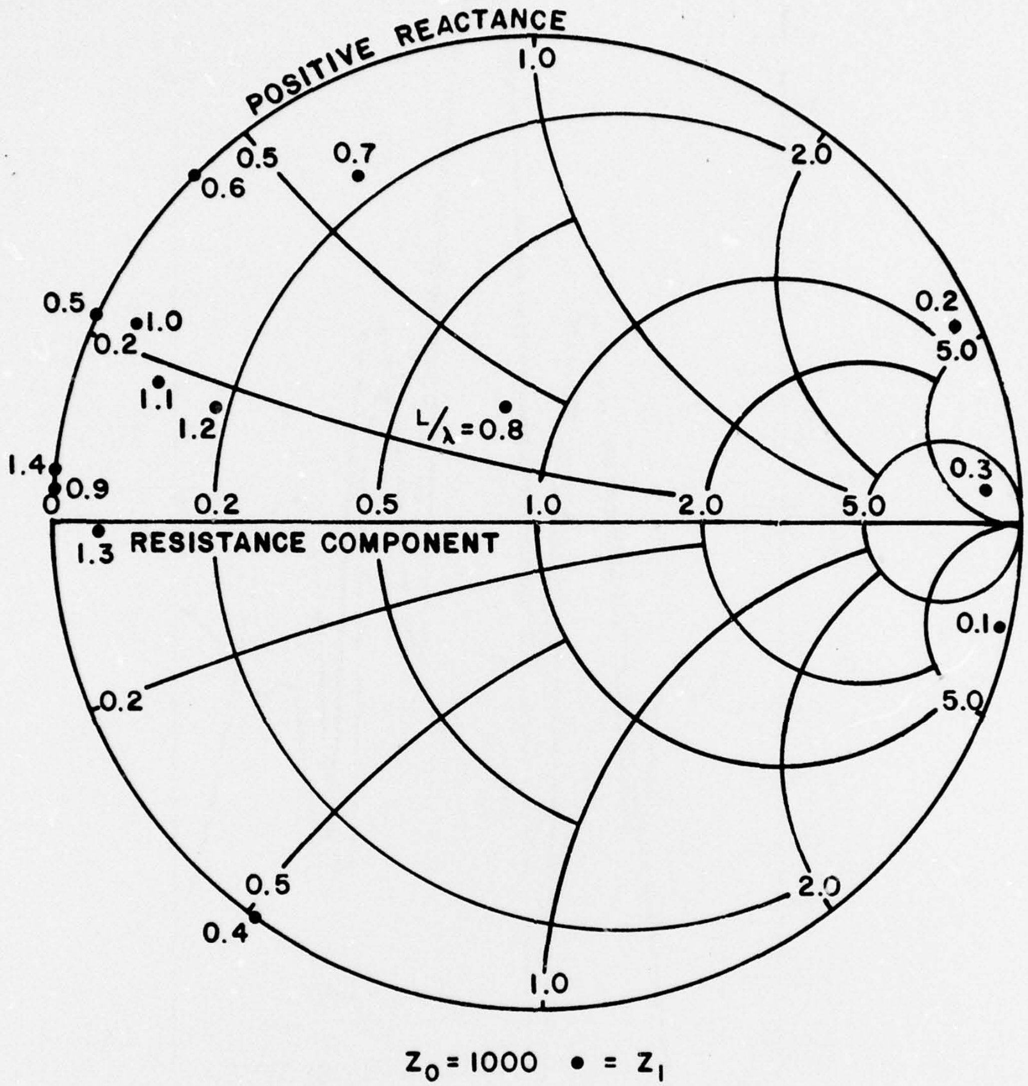

Figure 17. Values of Z_1 as function of L/λ.

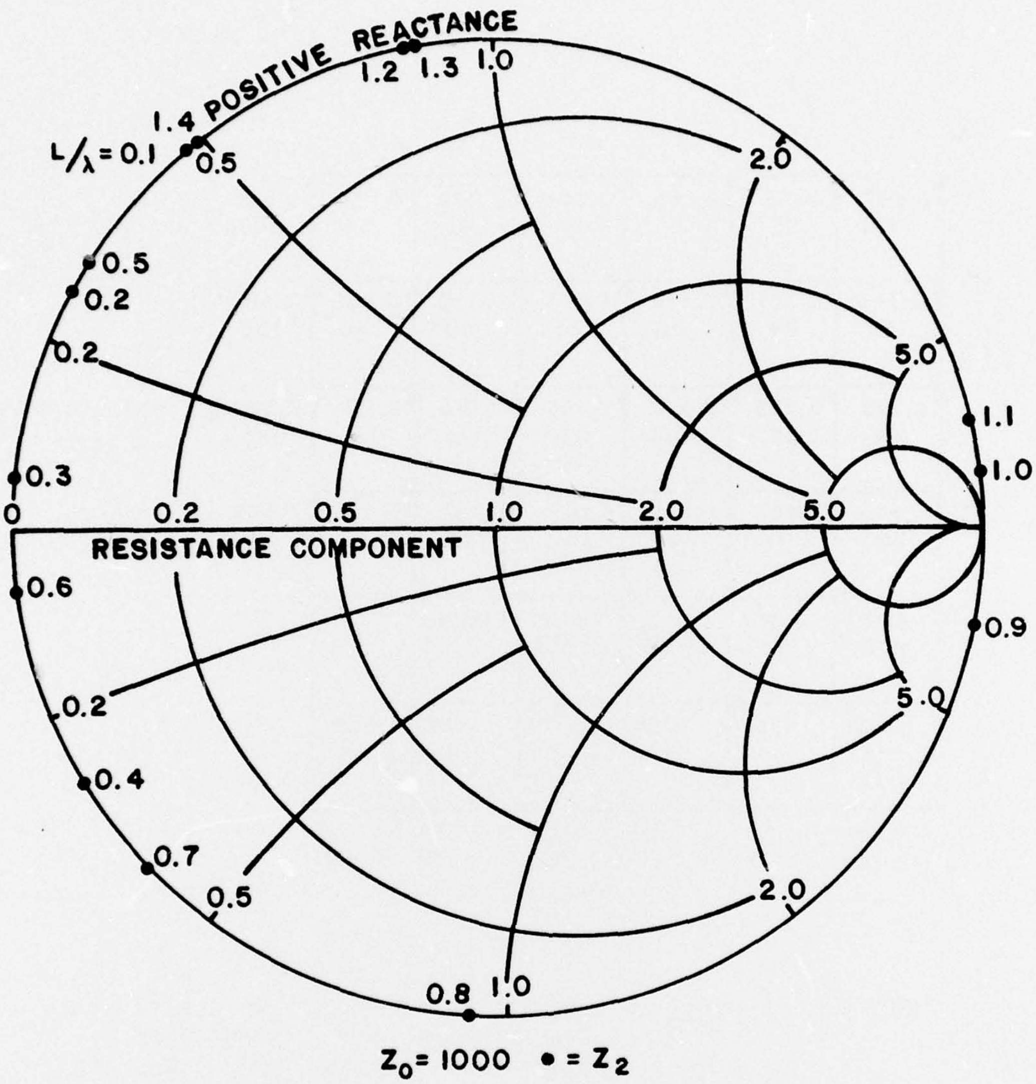

Figure 18. Values of Z_2 as function of L/λ.

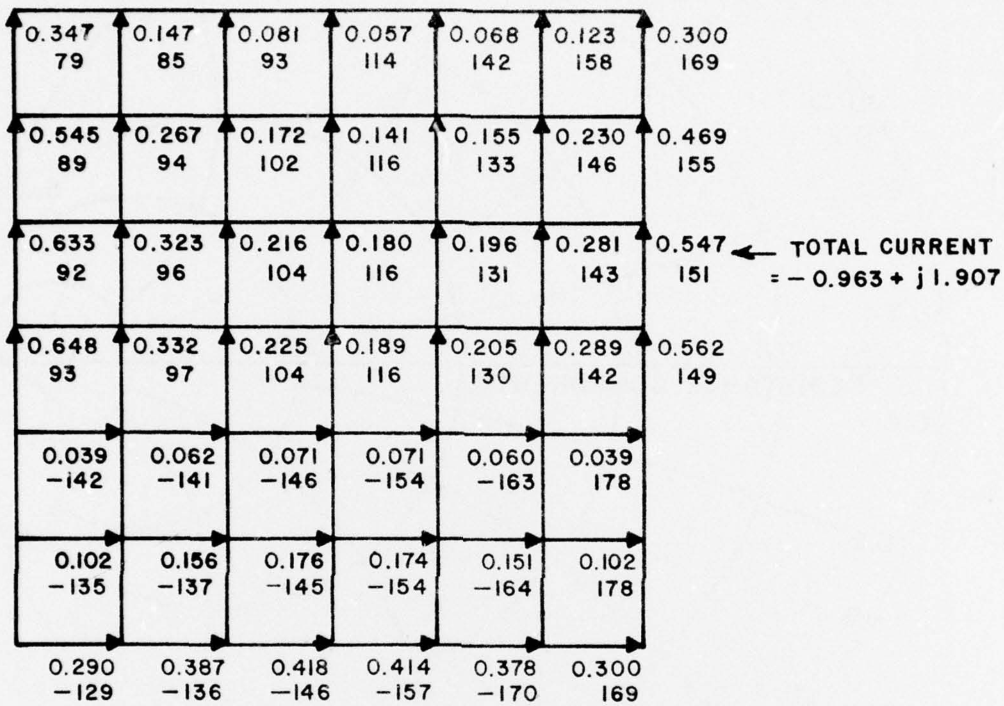

Figure 19. Current on a square plate of $L/\lambda = .2$ induced by a plane wave at grazing incidence. The upper number is the amplitude and the lower number is the phase in degree.

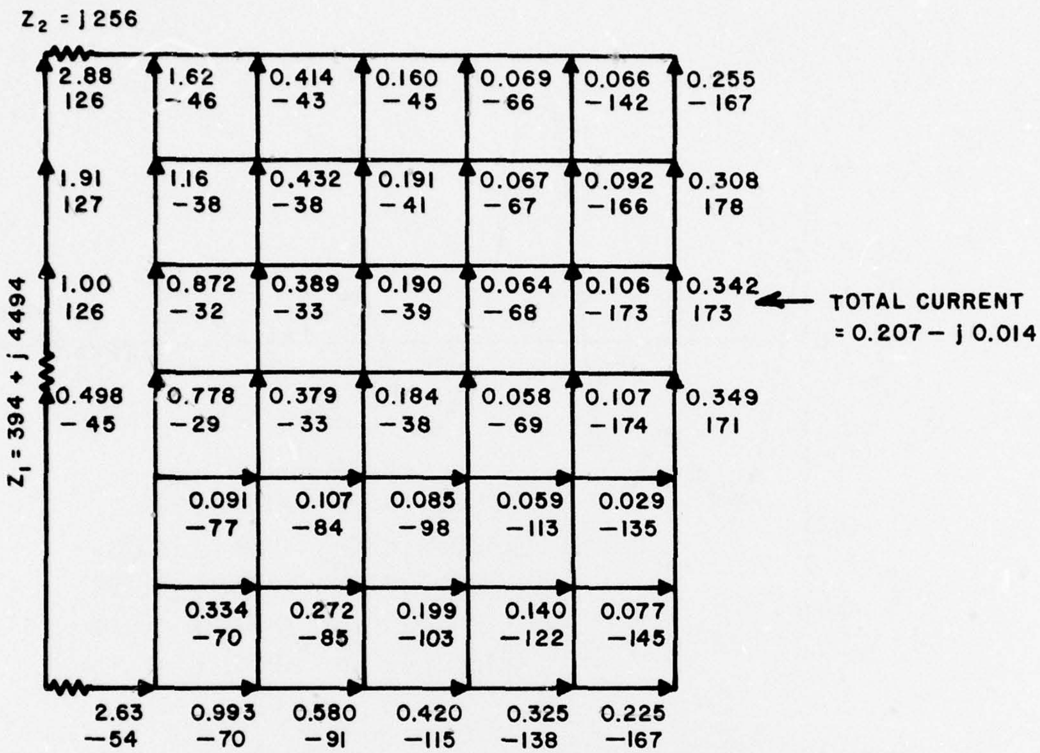

Figure 20. Current on a square plate of $L/\lambda=.2$ with optimal impedance loading induced by a plane wave at grazing incidence. The upper number is the amplitude and the lower number is the phase in degree.

as follows. With the unslotted plate Prony's method is applied to the endfire backscattered ramp response obtained via Fourier synthesis [7] and the dominant natural resonances are found to be $(-.515\pm j1.91)c/L$ where c is the velocity of light (Figure 21). Next the plate is slotted

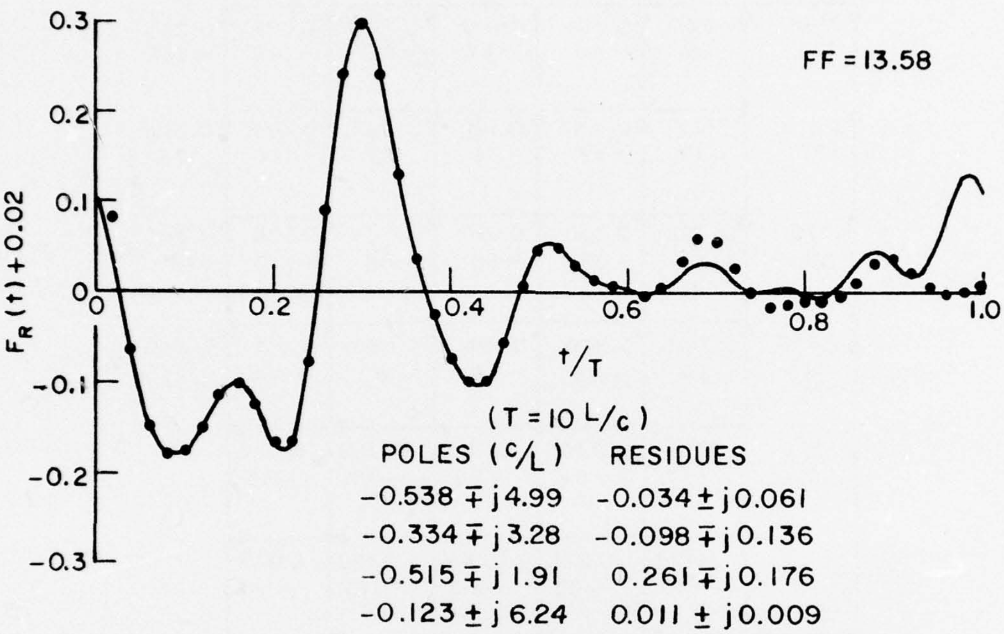

Figure 21. Endfire backscattered ramp response of a square plate.

and a fixed impedance $Z_1=200\Omega$ is inserted at the slotted edge. A slight change in the dominant natural resonances is found (Figure 22). At the dominant natural resonances of the unslotted plate the size of the plate is approximately $L/\lambda=.3$. If optimal impedances are obtained at this frequency which, from Figure 5, are found to be $Z_1=1600+j12500$, $Z_2=j42$ which can be made of some values of resistance and inductance, and if the values of resistance and inductance are kept constant, then the endfire backscattered ramp response is as shown in Figure 23. The dominant natural resonances have a much larger change from those of an unslotted plate. It should be noted that the ramp responses as shown in Figures 21 through 23 must be divided by the factor (FF) to obtain the true ramp responses. For comparison, the corresponding broadside backscattered ramp responses are shown in Figures 24 through 26. Comparing the first negative swing in Figures 24 through 26, it is seen that impedance loading has little effect on the specular scattering. This brief investigation is by no means complete, but does show that impedance loading technique for controlling nonspecular scattering may also find applications in target discrimination.

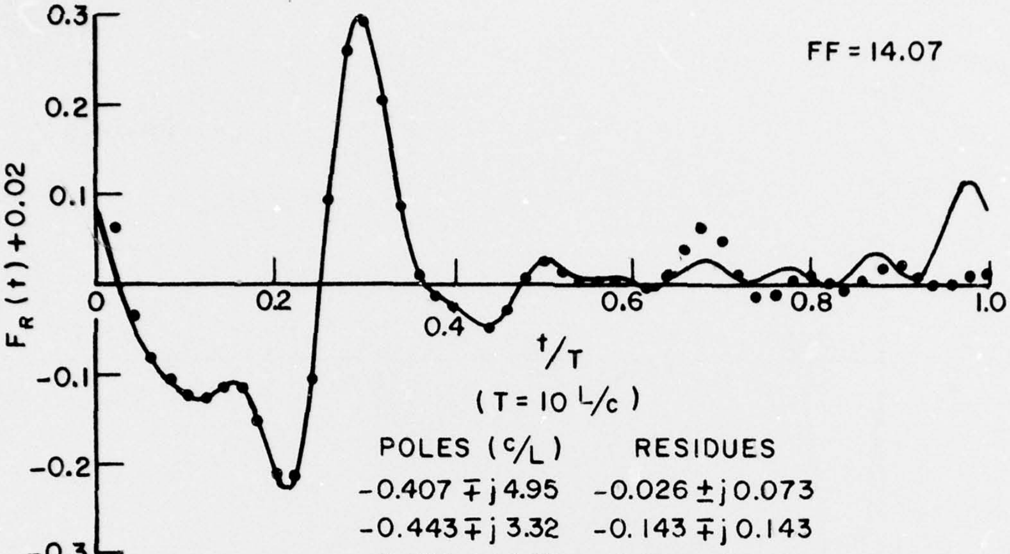

POLES (c/L)	RESIDUES
-0.407 ∓ j 4.95	-0.026 ± j 0.073
-0.443 ∓ j 3.32	-0.143 ∓ j 0.143
-0.574 ∓ j 1.85	0.276 ∓ j 0.175
-0.135 ± j 6.24	0.012 ± j 0.015

Figure 22. Endfire backscattered ramp response of a slotted square plate loaded with Z_1=200Ω.

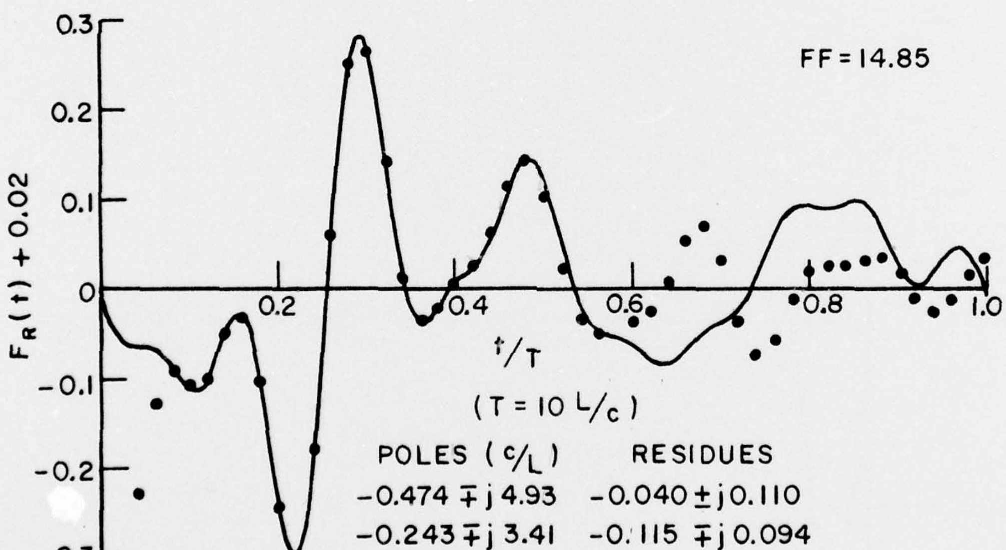

POLES (c/L)	RESIDUES
-0.474 ∓ j 4.93	-0.040 ± j 0.110
-0.243 ∓ j 3.41	-0.115 ∓ j 0.094
-0.437 ∓ j 1.09	-0.044 ∓ j 0.162
-0.163 ± j 6.20	0.008 ± j 0.034

Figure 23. Endfire backscattered ramp response of a slotted square plate loaded with impedances which are optimal at the frequency where L/λ=.3.

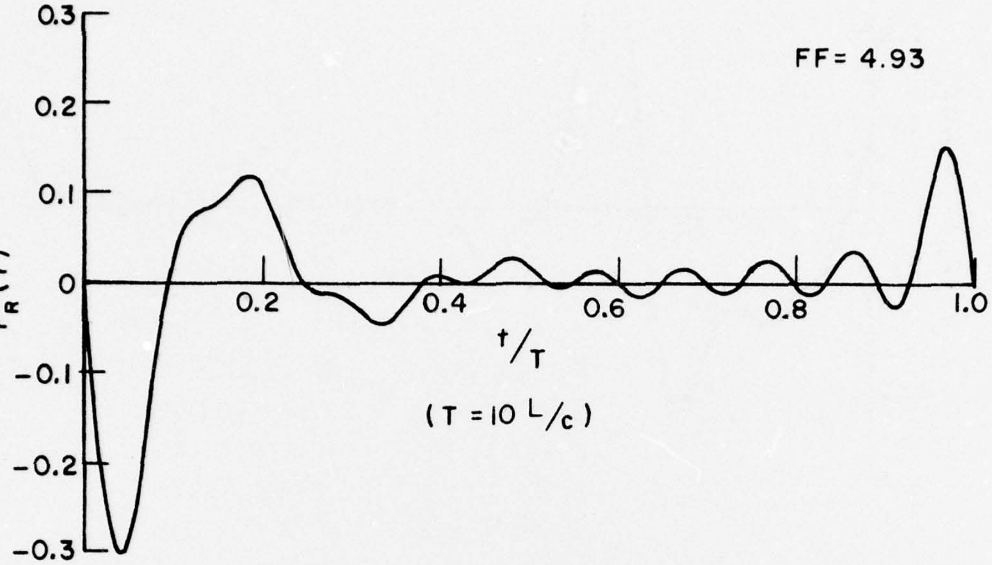

Figure 24. Broadside backscattered ramp response of a square plate.

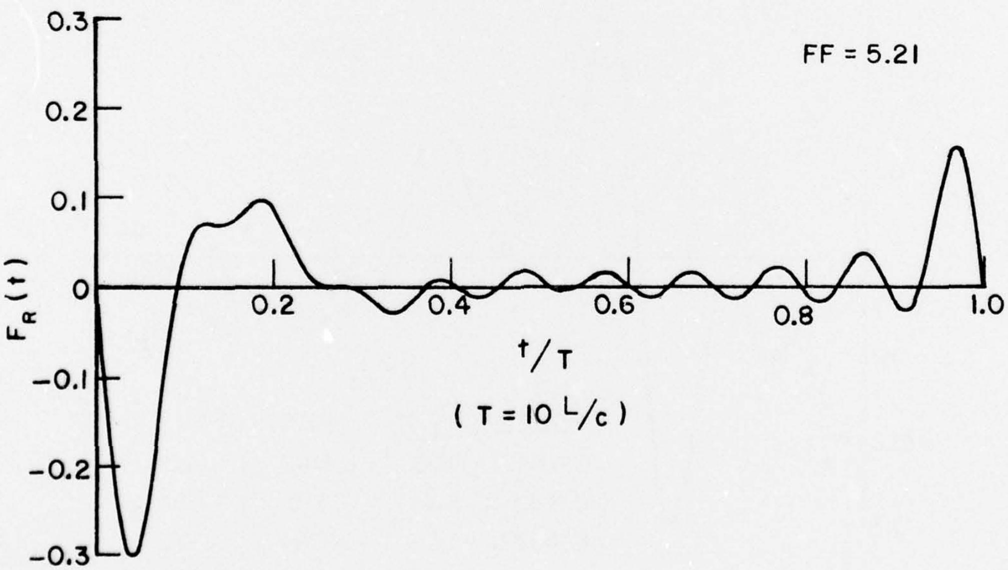

Figure 25. Broadside backscattered ramp response of a slotted square plate loaded with Z_1=200Ω.

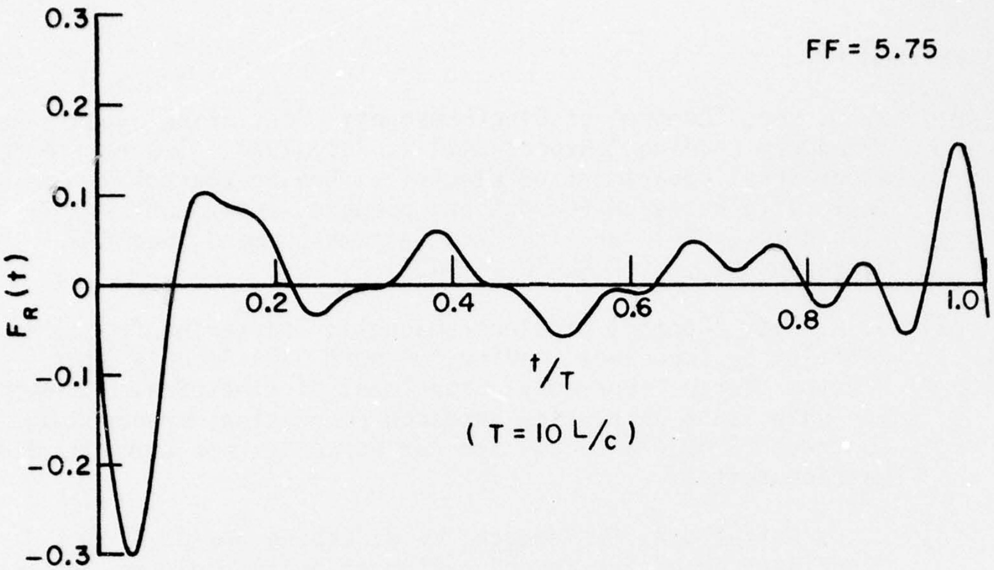

Figure 26. Broadside backscattered ramp response of a slotted square plate loaded with impedances which are optimal at the frequency where L/λ=.3.

VI. CONCLUSION

A generalized compensation theorem is derived in this report. The result is applied to the study of controlling backscatter from a thin square conducting plate by impedance loading. It is demonstrated that at near grazing incidence with the electric field polarized parallel to the leading edge of the plate, significant reductions of backscatter can be achieved for plate sizes ranging from L/λ=.1 to L/λ=1.4 with proper impedance loading. A similar study for the case of perpendicular polarization has been given in a previous report [1]. The main contributions of nonspecular backscatter for the two cases are different. For the former the leading edge of the plate contributes most of the backscatter and a properly loaded folded dipole is employed to reduce the backscatter. While for the latter the main contributor of the backscatter is the trailing edge and the backscattering reduction is accomplished through the use of a properly loaded slot. Comparison of the two studies shows that good backscattering reduction over a much larger bandwidth can be achieved for parallel polarization.

REFERENCES

[1] S. C. Lee, "Control of Electromagnetic Scattering by Antenna Impedance Loading," Report 3424-2, July 1974, ElectroScience Laboratory, Department of Electrical Engineering, The Ohio State University Research Foundation; prepared under Contract F19628-72-C-0203 for Air Force Systems Command, Bedford, Massachusetts. (AFCRL-TR-74-0426)

[2] J. A. Aas, "Control of Electromagnetic Scattering from Wing Profiles by Impedance Loading," Report 3424-4, July 1975, ElectroScience Laboratory, Department of Electrical Engineering, The Ohio State University Research Foundation; prepared under Contract F19628-72-C-0203 for Air Force Systems Command, Bedford, Massachusetts.

[3] D. L. Moffatt, R. C. Rudduck, C. W. Chuang and J. A. Aas, "Continuation of the Investigation of Multi-Frequency Radar Reflectivity and Radar Target Identification," Report 3424-5, July 1975, ElectroScience Laboratory, Department of Electrical Engineering, The Ohio State University Research Foundation; prepared under Contract F19628-72-C-0203 for Air Force Systems Command, Bedford, Massachusetts.

[4] J. H. Richmond, "Radiation and Scattering by Thin-Wire Structures in the Complex Frequency Domain," Report 2902-10, July 1973, ElectroScience Laboratory, Department of Electrical Engineering, The Ohio State University Research Foundation; prepared under Grant No. NGL36-008-138 for the National Aeronautics and Space Administration, Washington, D.C.

[5] J. H. Richmond, "Computer Program for Thin-Wire Antenna over a Perfectly Conducting Ground Plane," Report 2902-19, October 1974, ElectroScience Laboratory, Department of Electrical Engineering, The Ohio State University Research Foundation; prepared under Grant No. NGL36-008-138 for National Aeronautics and Space Administration, Washington, D.C.

[6] R. K. Mains and D. L. Moffatt, "Complex Natural Resonances of an Object in Detection and Discrimination," Report 3424-1, June 1974, ElectroScience Laboratory, Department of Electrical Engineering, The Ohio State University Research Foundation; prepared under Contract F19628-72-C-0203 for Air Force Systems Command, Bedford, Massachusetts. (AFCRL-TR-74-0282).

[7] C. W. Chuang and D. L. Moffatt, "Complex Natural Resonances of Radar Targets via Prony's Method," Report 3424-3, April 1975, ElectroScience Laboratory, Department of Electrical Engineering, The Ohio State University Research Foundation; prepared under Contract F19628-72-C-0203 for Air Force Systems Command, Bedford, Massachusetts. (AFCRL-TR-75-0203)

MISSION
of
Rome Air Development Center

RADC plans and conducts research, exploratory and advanced development programs in command, control, and communications (C^3) activities, and in the C^3 areas of information sciences and intelligence. The principal technical mission areas are communications, electromagnetic guidance and control, surveillance of ground and aerospace objects, intelligence data collection and handling, information system technology, ionospheric propagation, solid state sciences, microwave physics and electronic reliability, maintainability and compatibility.

AMERICAN REVOLUTION BICENTENNIAL 1776-1976

Printed by
United States Air Force
Hanscom AFB, Mass. 01731